Journal of Thermal Analysis and Calorimetry, Vol. 71 (2003) 773–782

EMANATION THERMAL ANALYSIS STUDY OF SYNTHETIC GIBBSITE
Evaluation of experimental ETA results by mathematical modelling

V. Balek[1*], *J. Šubrt*[1], *J. Rouquerol*[2], *P. Llewellyn*[2], *V. Zeleňák*[3], *I. M. Bountsewa*[4], *I. N. Beckman*[4] *and K. Györyová*[3]

[1]Institute of Inorganic Chemistry, Academy of Sciences of the Czech Republic, 250 68 Řež, Czech Republic
[2]MADIREL, UMR CNRS - Provence University, Centre de St Jérôme, 13397 Marseille, Cedex 20, France
[3]Institute of Chemical Sciences, Department of Inorganic Chemistry, Faculty of Sciences, P. J. Šafárik University, 041 54 Košice, Slovak Republic
[4]Chemical Faculty, Moscow State University, 119899 Moscow, GSP-3, Russia

Abstract

Emanation thermal analysis (ETA) was used for thermal characterization of microstructure changes taking place during heating of synthetic gibbsite sample in argon in the range of 25–1200°C. Microstructure development and the increase of the surface area under *in-situ* conditions of the sample heating were characterized. The increase of the radon release rate from 130–330°C monitored the increase of the surface area due to the dehydration of $Al(OH)_3$. During heating of the sample in the range 450–1080°C the ETA results characterized the annealing of surface and near surface structure irregularities of intermediate products of gibbsite heat treatment. The mathematical model for the evaluation of the ETA experimental results was proposed. From the comparison of the experimental ETA results with the model curves it followed that the model is suitable for the quantitative characterization of microstructure changes taking place on heating of gibbsite sample.

Keywords: ETA, gibbsite, mathematical modelling, microstructure changes

Introduction

Thermal behaviour of aluminium hydroxide, called gibbsite, was investigated both as natural and synthetic mineral by a number of authors [1–13]. Thermogravimetry (TG), differential thermal analysis (DTA), XRD, IR-spectroscopy and other techniques were used to elucidate the mechanism of the thermal behaviour of gibbsite under different conditions including the effect of mechanochemical activation [14–18].

It was shown by Rouquerol *et al.* [10, 19], by using a form of controlled rate thermal analysis (CRTA) which we now call controlled rate evolved gas detection (CR-EGD),

* Author for correspondence: E-mail: bal@ujv.cz

1388–6150/2003/ $ 20.00
© 2003 Akadémiai Kiadó, Budapest
Akadémiai Kiadó, Budapest
Kluwer Academic Publishers, Dordrecht

that microporous alumina with tailored porosity can be prepared by thermal decomposition of gibbsite under controlled low pressure of the residual water vapour.

The aim of this study was to characterize by means of ETA [20, 21] the microstructure changes taking place during heating of the synthetic gibbsite in argon and to evaluate the experimental ETA results by using a mathematical model. The ETA results were compared with the results of TG and DTA.

Experimental

Material studied

A synthetic gibbsite $Al(OH)_3$ obtained by the Bayer process and supplied by Pechiney (France) was used in the experiment. Its grain size is between 50 and 80 μm, its krypton BET surface area is 0.14 m^2 g^{-1} and it contains 0.21% sodium, 0.08% iron and 0.21% CO_2.

Methods used

ETA [20, 21] involves the measurements of radon release rate from samples previously labelled. The samples for ETA were labelled by acetone solution containing traces of ^{228}Th and ^{224}Ra nitrates. The specific activity of a sample after labelling was

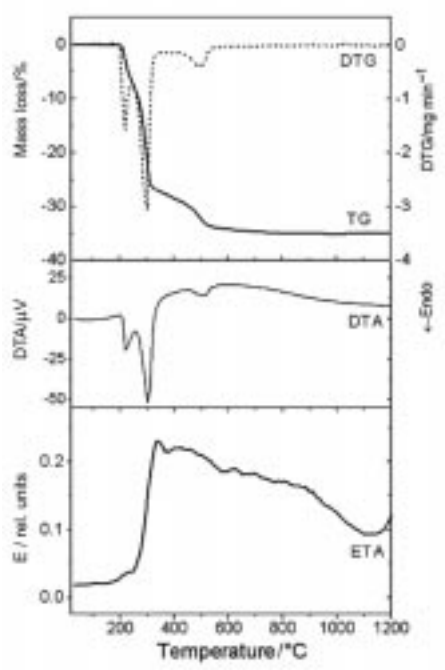

Fig. 1 TG/DTG, DTA and ETA results of gibbsite measured during heating in argon at the rate 6 K min^{-1}

10^5 Bq g^{-1}. Atoms of ^{220}Rn were formed by the spontaneous α-decay of ^{228}Th and ^{224}Ra. The ^{224}Ra and ^{220}Rn atoms were incorporated into the sample due to the recoil energy (85 keV/atom), which the atoms gain by the spontaneous α-decay. The maximum depth of ^{220}Rn penetration was calculated by TRIM code [22]. It was determined that the surface and near surface layers up to the maximal depth of 80 nm were labelled. The values of the radon release rate E (in relative units) were calculated from the measured radioactivity values A_α of the Rn atoms released from the sample, divided by the total radioactivity of the parent nuclides A_γ used for the sample labelling i.e. $E=A_\alpha/A_\gamma$ as described in [20]. Semiconductor detector was used for the measurement of the total γ-radioactivity. The schematic drawing of the ETA part of the apparatus is given as Fig. 1 in [20].

The ETA measurements were performed during heating in argon at the rate of 6 K min^{-1}, using a modified Netzsch ETA-DTA instrument, model 404. During the ETA measurements the labelled sample of 0.1 g was situated in a corundum crucible and overflowed with the constant flow of argon (flow rate 50 cm^3 min^{-1}), which carried the radon released from the sample into the measuring chamber of radon radioactivity. Details of the ETA measurements and data treatment has been described elsewhere [20].

TG-DTA measurements were carried out using NETZSCH STA 409 apparatus in the flow of argon (flow rate 50 cm^3 min^{-1}). The sample mass was 0.1 g, the sample was placed into corundum crucible and heated at the rate of 6 K min^{-1}.

Results and discussion

TG/DTG, DTA and ETA results

Figure 1 presents the TG/DTG, DTA and ETA results of synthetic gibbsite obtained during heating in argon. The total mass loss observed on TG curve in the temperature range 220–820°C was 34.2%. This value is in agreement with the theoretical value 34.6% for the reaction (1). The dehydration of the sample was characterized by three DTA endothermic effects at 222, 303 and 498°C.

$$Al(OH)_3 \rightarrow 1/2Al_2O_3+3/2H_2O \quad (1)$$

These DTA peaks were interpreted by several authors [1–4] who agree on the general interpretation although not on the more detailed mechanism. For instance, the first peak, observed here at 222°C, is usually considered to correspond to a partial transformation of gibbsite into boehmite, according to the Scheme (2) given by Mackenzie:

$$Al(OH)_3 \rightarrow \chi\text{-}Al_2O_3+\gamma\text{-}AlO(OH) \quad (2)$$

Now, it looked logical to most authors that the transformation starts on the surface of the gibbsite crystal. Nevertheless, Rouquerol *et al.* [9] showed that this step did not correspond to any increase in the krypton or nitrogen BET surface area (hence no transition alumina is formed in the outer parts of the crystal) whereas droplets of free water were shown (by NMR) to develop in the core of the crystal: this leads to the idea that boehmite is formed in the center of the crystal, where hydrothermal con-

ditions favourable to this transformation exist, and that this boehmite (which is 23% denser than the starting gibbsite) leaves room for small cavities (located in the core of the boehmitic phase) able to accomodate, in standard liquid form, part of the water produced by reaction (2).

This first endothermic DTA peak corresponds to a mass loss of ~7.4% (TG curve in Fig. 1). The second, more intense endothermic peak at 303°C, was accompanied by a mass loss of ~22.1%.

A further mass loss of ~5.1% was completed at 820°C and corresponds to the total dehydration of boehmite and formation of a second type of anhydrous aluminium oxide. The latter dehydration step can be formally expressed by the chemical reaction (3).

$$AlO(OH) \rightarrow 1/2Al_2O_3 + 1/2H_2O \quad (3)$$

This transformation is reflected by the endothermic effect on DTA curve at 498°C. The temperature of this effect is in accordance with the temperature of dehydroxylation of boehmite, stated by Mackenzie [8].

The ETA characterized microstructure development of the sample and brought about additional information about microstructure development under *in-situ* conditions of heating. The ETA results in Fig. 1 enabled us to determine the temperature intervals at which the microstructure changes, due to respective dehydration steps took place in comparison with the results of TG and DTA.

The microstructure changes which accompanied the first step of the dehydration (reflected by the DTA effect at 222°C) were reflected by ETA as a small effect only, in the same temperature range. The observed small intensity of the effect was in agreement with the mechanism of the dehydration of gibbsite proposed by Rouquerol [10, 19]. He suggested that the first step of the gibbsite dehydration takes place in the core of the grains under hydrothermal conditions. Taking into account that the gibbsite crystals were labelled by ^{220}Rn and its ^{224}Ra parent nuclide to the maximum depths of the 80 nm, the information obtained by ETA must be considered as the description of behaviour of surface layers up to this depth. Consequently, from the observed small ETA effect it was assumed no drastic microstructure changes took place in this near surface layers of the gibbsite sample in the mentioned temperature range. This confirmed the hypothesis published in [10, 19] that the water formed during the dehydration of gibbsite escaped from the crystal through very narrow 'structural channels' formed in the gibbsite structure. These channels are parallel to each other and perpendicular to the reaction interface [19]. We supposed that the surface area acting at this dehydration was much smaller in comparison to the surface area of the whole crystal. Consequently, only small increase of the radon release rate could be observed on ETA in the temperature range 200–260°C.

The steep increase of the radon release rate observed on sample heating from 230 to 333°C indicated drastic microstructure changes which took place in this temperature range as the result of rupture of the core on the particle surface and that water was released through overall surface of the grains. This gave rise to the large surface area of the intermediate product and formation of new paths for radon release from the sample.

From the break observed at 330°C on the ETA curve and the subsequent decrease of the radon release rate, E, it followed that the surface area of the intermediate

products slightly decreased on heating in spite of the fact that the dehydration of the AlO(OH) continued in this temperature range and formation of Al_2O_3 was indicated by DTA endothermic effect at 498°C: this is well in agreement with the earlier finding that the transition alumina produced has relatively low thermal stability and starts to loose its nitrogen BET surface area at 300°C under 5 mbar [19].

The decrease of E in the temperature range 615–1100°C reflected the decrease of surface area and annealing of near surface structure irregularities in anhydrous Al_2O_3. The enhanced increase of radon release rate E above 1100°C was ascribed to the diffusion of the radon atoms from bulk of the sample.

Mathematical modelling and evaluation of ETA results

It was supposed in the modelling that ^{228}Th and ^{224}Ra do not migrate in the solid at the temperatures used for the ETA measurements. The value of the total emanating rate E_{TOTAL} of a solid is composed of two terms, namely the emanating rate, E_R, due to recoil, and the emanating rate, E_D, due to diffusion. The emanating rate E_R depends on the shape and size of the sample, the recoil range of ^{224}Ra and ^{220}Rn in the sample and on the initial distribution of ^{228}Th.

According to the theory proposed recently by Beckman and Balek [23], the total emanating rate, E, during solid-state transitions of solids can be schematically written as:

$$E(T)=E_R+E_D(T)\Psi(T) \quad (4)$$

i.e. the second term is a product of two functions; E_D characterizing the radon permeability of diffusion channels and the $\Psi(T)$ function characterizing the microstructure changes in the solid.

In Fig. 2 the experimental ETA results (presented as dots) are compared with the temperature dependences of radon release rate obtained by modelling (curves 2–4). It was supposed, that following chemical processes took place in course of heating of

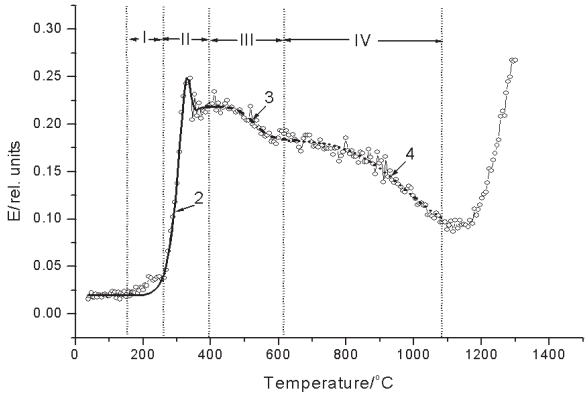

Fig. 2 Comparison of experimental ETA results (dots) with the results of the mathematical modelling (curves 2–4) of the radon release rate from the gibbsite sample in segments II–IV. Segments I–IV were determined considering, that in each segment only one type of solid-state change to be described by mathematical modelling takes place

gibbsite: the dehydration gibbsite to boehmite AlO(OH) and the dehydration of boehmite AlO(OH) to aluminium oxide Al_2O_3, both accompanied by release of remaining water from the sample. Therefore the model of parallel diffusion was used for the description of radon mobility in the synthetic gibbsite and the products of its thermal decomposition. Four temperature ranges were distinguished during the modelling of the ETA curve (Fig. 2 and Table 1).

In the ranges I and II, i.e. from 130 to 270°C and from 270 to 395°C, respectively Eqs (5)–(7) were used in the modelling:

$$E_1(T)=E_{1D}(T)*\Psi_1(T) \tag{5}$$

where

$$E_{ID}(T)=p1\,p2\exp\left(-\frac{p3}{T}\right)\left[\coth\left(\frac{3}{p\mathrm{lexp}\left(-\frac{p3}{T}\right)}\right)-\frac{p\mathrm{lexp}\left(-\frac{p3}{T}\right)}{3}\right] \tag{6}$$

and

$$\psi_1(T)=1-\frac{p4}{2}\left[1+\mathrm{erf}\left(\frac{T-p5}{\sqrt{2}\,p6}\right)\right] \tag{7}$$

In the ranges III and IV i.e. from 400 to 615°C and from 615 to 1080°C, respectively the Eqs (8) and (9) were used for the modelling:

$$E_2(T)=\Psi_2(T) \tag{8}$$

where

$$\psi_2(T)=p7\left\{1-\frac{p4}{2}\left[1+\mathrm{erf}\left(\frac{T-p5}{\sqrt{2}\,p6}\right)\right]\right\} \tag{9}$$

and $p1$–$p7$ are parameters. In the calculation of these parameters we assumed that the process of dehydration and structure defects annealing can be formally described as first order kinetics.

From the parameters obtained during the modelling, the activation energy Q_D [J mol^{-1}] of radon diffusion as well as enthalpy ΔH [J mol^{-1}] of the solid-state processes were calculated:

$$Q_D=2Rp3\ [\mathrm{J\ mol^{-1}}] \tag{10}$$

where R molar gas constant

$$\Delta H(T)=T_{\max}\left[69.5+4.6\log_{10}\left(\frac{T_{\max}}{\beta}\right)\right][\mathrm{J\ mol^{-1}}] \tag{11}$$

The T_{max}=$p5$ corresponds to the temperature of the maximal rate of the solid-state process. The calculated values of the activation energy Q_D of radon diffusion as well as enthalpy ΔH the solid-state process in the respective temperature intervals are given in Table 1.

Table 1 The values of the activation energy Q_D/J mol^{-1} of radon diffusion and enthalpy ΔH/J mol^{-1} of the structural process in the respective temperature intervals

Temp. interval of the ETA curve/°C	I 130–270	II 270–395	III 395–615	IV 615–1080
Onset and final temperature of microstructure changes determined from $\Psi_i(T)$ function/°C	130 340	310 370	430 615	615 1100
Q_D/J mol^{-1}	$1.541 \cdot 10^5$	$2.396 \cdot 10^5$	–	–
ΔH/J mol^{-1}	$4.126 \cdot 10^4$	$4.504 \cdot 10^4$	$6.358 \cdot 10^4$	$9.98 \cdot 10^4$
T_{max}/°C	253	338	529	972
$\frac{\Psi_i(T)_{max}}{\psi(T)}$/%	1	3.5	3	10.2

The comparison of the experimental ETA results with the results of the mathematical modelling for the dehydration of gibbsite in the range up to 1100°C is presented in Fig. 2.

In order to quantitatively describe microstructure changes taking place during heating of gibbsite in the investigated temperature ranges, we selected four segments (Fig. 2) supposing for each segment the existence of one type of solid-state change. In the segment I (from 130 to 270°C) no remarkable effect corresponding to microstrure changes in the near surface layers of gibbsite during dehydroxylation was observed, in the segment II (from 270 to 395°C) the surface area increased, characterizing the drastic microstructure changes as the result of rupture of the core on the surface of the decomposing gibbsite particles, in the segment III (from 400 to 615°C) and IV (from 615 to 1080°C) the annealing of surface and near surface layers of the intermediate product of thermal decomposition were supposed.

The model curve 2 in Fig. 2 characterized the rupture of the core on the surface of the particles and the water release through all the surface of the grains. The activation energy Q_D of radon diffusion as well as enthalpy ΔH during this solid-state process, which were calculated using the proposed model are 239.6 and 45.04 kJ mol^{-1}, respectively. The model curve 3 in Fig. 2 characterized the final step of the sample dehydration. The decrease of the radon release rate reflected the fact that the surface area of boehmite did not increase during heating in spite of the fact that the dehydration of the γ-AlO(OH) continued. The calculated enthalpy ΔH of this process is 63.58 kJ mol^{-1}. Model curve 4 in Fig. 2 characterized the decrease of surface area and annealing of near surface structure irregularities in anhydrous Al_2O_3. The calculated value of enthalpy characterizing this process is 99.8 kJ mol^{-1}.

In addition, in order to better characterize the process of formation of boehmite under hydrothermal conditions, which was reflected as a small effect on experimental ETA curve, the modelling of the experimental ETA results in segment I was carried out separately.

The model curves 2–4 were subtracted from the experimental ETA curve and curve presented in Fig. 3 as dots resulted. The result of the mathematical treatment of these data is presented in Fig. 3 as curve 1. The following values of activation energy of radon diffusion Q_D and enthalpy ΔH of this solid-state process were determined from the modelling: Q_D=154.1 and ΔH = 41.26 kJ mol^{-1}, respectively.

The $\Psi_i(T)$ functions used in the mathematical modelling for the characterization of the microstructure changes and/or the annealing of radon diffusion paths in the gibbsite sample in the above determined four segments are presented in Fig. 4. The functions $\Psi_i(T)$ (curves 1–4) as well as their first derivatives $d\Psi_i/dT$ (curves 1'–4')

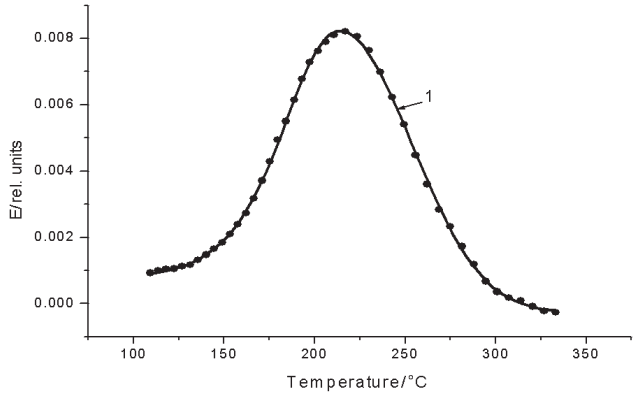

Fig. 3 Results of mathematical modelling (curve 1) compared with the experimental ETA data (dots) characterizing microstructure changes in segment I

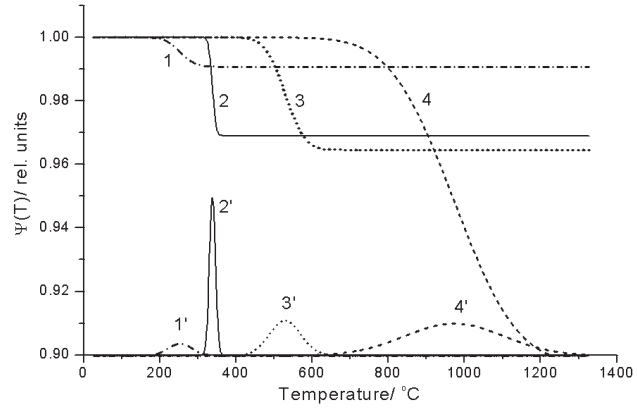

Fig. 4 Temperature dependences of functions $\Psi_i(T)$ (curves 1–4) and their derivatives $d\Psi_i/dT$ (curves 1'–4') in different segments of ETA curves as determined in Fig. 2

were used for the evaluation of the microstructure changes in the individual segments determined in Fig. 2. The temperatures of T_{max}, which indicate the maximal rate of the annealing of radon diffusion paths, were determined from the curves 1'–4' in Fig. 4 and are summarized in Table 1 along with the values of the parameter $\Psi_i(T)\max/\Psi(T)$ characterizing the relative intensity of the annealing processes in the respective segments. From Fig. 4 it follows that the lowest intensity of the microstructure changes was observed in the temperature range from 130 to 270°C, whereas the relative highest intensity (more than 10%) corresponds to the change above 615°C characterizing the annealing of alumina particles.

Conclusions

ETA results brought about additional information about development of the microstructure during thermal decomposition of gibbsite. The mathematical model used for the evaluation of ETA experimental results was found suitable and can be recommended for further application.

* * *

The results were supported by the Ministry of Education of the Czech Republic in the frame of the projects No LN00A028 and ME 344 (Program Kontakt). The authors thank for the financial support of the bilateral cooperation between Czech Republic and France (Barrande project, No 2000-014). The authors (I.M.B and I.N.B) express their thanks to NATO science fellowship programme for the financial support of the research stay in the Czech Republic.

References

1 R. C. Mackenzie, in 'The Differential Thermal Investigation of Clays' (R. C. Mackenzie, Ed.) Mineralogical Society, London 1957, p. 299.
2 W. F. Bradley and R. E. Grim, Am. Miner., 36 (1951) 182.
3 J. F. Brown, D. Clark and W. W. Elliott, J. Chem. Soc. London, 13 (1953) 84.
4 J. H. de Boer, J. M. H. Fortuin and J. J. Steggerda, Proc. Kon. Ned. Akad. Wetensch., Ser. B 57 (1954) 170.
5 V. P. Ivanova, Zap. vses. Miner. Obshch., 90 (1961) 50.
6 B. A. Scott and W. H. Horsman, Trans. Brit. Ceram. Soc., 69 (1970) 131.
7 W. Lodding, in 'Thermal Analysis', R. F. Schwenker Jr. and P. D. Garn Eds, Academic Press, New York 1969, p. 1249.
8 R. C. Mackenzie, in 'Differential Thermal Analysis' Vol. I., (R. C. Mackenzie, Ed.), Academic Press, London 1970, p. 279.
9 J. Rouquerol, F. Rouquerol and M. Ganteaume, J. Catal., 36 (1975) 99.
10 J. Rouquerol, F. Rouquerol and M. Ganteaume, J. Catal., 57 (1979) 222.
11 F. Paulik, J. Paulik and R. Nauman, Thermochim. Acta, 64 (1983) 1.
12 K. J. D. MacKenzie, J. Thermal Anal., 5 (1973) 19.
13 R. C. T. Slade, J. C. Southern and I. M. Thompson, J. Mater. Chem., 1 (1991) 563.
14 J. T. Kloprogge, H. D. Ruan and R. L. Frost, J. Mater. Sci., 37 (2002) 1121.

15 M. N. Danchevskaya, O. G. Ovchinnikova, Y. D. Ivakin and G. P. Muraveva, Russ. J. Phys. Chem., 74 (2000) 1250.
16 A. P. Ilin, V. Y. Prokofev, T. V. Sazanova and S. P. Kochetkov, Russ. J. Appl. Chem., 70 (1997) 93.
17 U. Steinike, H. Geissler, H. P. Hennig, K. Jancke, J. Jedamzik, U. Kretzschmar and U. Bollmann, Z. Anorg. Allg. Chem., 590 (1990) 213.
18 K. J. D. MacKenzie, J. Temuujin and K. Okada, Thermochim. Acta, 327 (1999) 103.
19 J. Rouquerol and M. Ganteaume, J. Thermal Anal., 11 (1977) 201.
20 V. Balek, Thermochim. Acta, 192 (1991) 1.
21 V. Balek, J. Šubrt, T. Mitsuhashi, I. N. Beckman and K. Györyová, J. Therm. Anal. Cal., 67 (2002) 15.
22 J. F. Ziegler and J. P. Biersack, The stopping and range of ions in solids, Pergamon Press, New York 1985.
23 I. N. Beckman and V. Balek, J. Therm. Anal. Cal., 67 (2002) 49.